Transition-Metal Host Complexes Designed for Critical-Locus Accommodation of Organic Guest Molecules—An Approach to a New Kind of Coordination Catalysts Patterned after Enzymes

Kenneth J. Takeuchi,[†] Daryle H. Busch,*[†] and Nathanial Alcock[‡]

Contribution from the Chemistry Departments, The Ohio State University, Columbus, Ohio 43210, and University of Warwick, Coventry, CV4 7 AL, England.
Received August 23, 1982

Abstract: A family of macrobicyclic ligands has been designed as prototypes of a new class of coordination catalysts. The ligand simultaneously chelates to a metal ion, thereby creating a reactive site, and also serves as host in inclusion complex formation with a potential substrate which acts as a guest. Thus the substrate must be held in critical locus to the active site. The new family of *vaulted* complexes are designed to facilitate dioxygen binding to cobalt(II) and iron(II) while accommodating an organic guest in a large permanent void. X-ray and NMR studies show that the nickel(II) complexes have the expected commodious void and that they can be expected to form inclusion complexes by hydrophobic interactions.

Cyclodextrins are the first[1] and most extensively studied[2] of all host compounds. The cyclic oligosaccharides are highly soluble in water and form inclusion complexes with many guest species ranging from polar acids, amines, and anions to apolar aliphatic and aromatic hydrocarbons. They have played a central role in the development of techniques for the study of guest–host complexing, and X-ray structure results on a number of their complexes[3-5] provide assurance as to the general nature of the interaction.

Inclusion complex formation[6] is recognized as occurring when the host includes the guest without covalent bond formation. According to Cram,[7] the host is characterized by its employment of converging binding sites while the guest uses diverging binding sites. These relationships are most clear with such hosts as macrocyclic polyethers, cryptates,[8] spherands,[9] or similar structures designed to express chiral recognition.[10] In addition to such polar interactions as hydrogen bonds and dipole–dipole attractions, hydrophobic or apolar phenomena may be involved in guest–host complexation.

The cyclophanes, polycyclophanes, and cyclodextrins possess large lipophilic voids which can provide refuge for hydrophobic guest substrates from the effects of solvent in aqueous media. Murakami[11] demonstrated such hydrophobic interactions for the paracyclophane of structure I through studies on the promotion of hydrolysis of alkyl *p*-nitrophenyl esters. Tabushi[12] synthesized several polycyclophane compounds containing heteroatoms, typically involving four 1,4-disubstituted benzene rings (structure II, X = S or N). Evidence was provided for guest–host complexing both in solution and in the solid state.[12,13] Particular attention is focused here on guest–host interactions resulting from hydrophobic interactions because this is inferred to be the source of enzyme–substrate binding[14,15] in the powerful oxidizing enzymes cytochromes P450.

The complexes reported here were designed as prototypic of a new class of transition-metal catalysts which feature both the presence of a metal-centered reactive site and an accommodation for substrate binding; i.e., guest–host complexing. The well-known behavior of cyclochromes P450 illustrates the basic requirements for related oxygenation catalysts. In the enzyme system, two complexation preequilibria precede the crucial event, the substrate oxygenation: (1) the enzyme and substrate form a complex and (2) after reduction of iron(III) to iron(II), dioxygen binds to the metal ion. While further requirements are recognized for successful catalysis in these systems, we address only these preequilibria at this time.

In earlier reports, we have shown that the ligands of structures III and IV, the lacunar-1 and lacunar-2 structures, produce

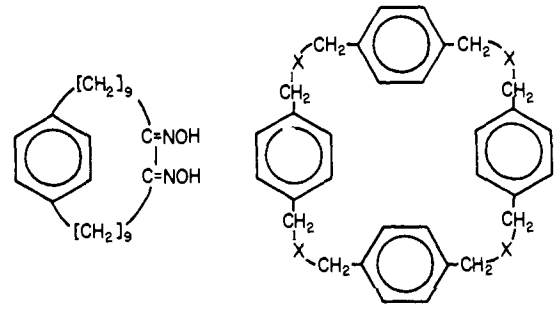

I II

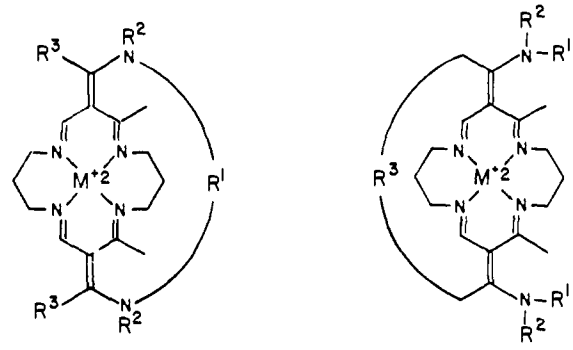

III IV

iron(II)[16-18] and cobalt(II)[18-21] complexes hving exceptional dioxygen-binding capabilities. We have chosen the lacunar-1 ligands

[†] The Ohio State University.
[‡] University of Warwick.

(1) Freudenberg, K.; Cramer, F. *Z. Naturforsch., B: Anorg. Chem., Org. Chem., Biochem., Biophys., Biol.* **1948**, *B3*, 464.
(2) Bender, M.; Kamiyama, M. "Cyclodextrin Chemistry. Reactivity and Structure Concepts in Organic Chemistry"; Springer-Verlag: Berlin, 1978; Vol 6, and references therein.
(3) Saenger, W.; McMullan, R.; Rayos, R.; Mootz, D. *Acta Crystallogr., Sect. B.* **1974**, *B30*, 2019.
(4) Harata, K.; Uedaira, H. *Nature (London)* **1975**, *253*, 190.
(5) Harata, K.; Uedaira, H.; Tanaka, J. *Bull. Chem. Soc. Jpn.* **1978**, *51*, 1627.
(6) Saenger, W. *Angew. Chem., Int. Ed. Engl.* **1980**, *19*, 344.
(7) Cram, D. J.; Cram, J. M. *Acc. Chem. Res.* **1978**, *11*, 8.
(8) Lehn, J.-M. *Acc. Chem. Res.* **1978**, *11*, 49.
(9) Trueblood, K. N.; Knobler, C. B.; Maverick, E.; Helgeson, R. C.; Brown, S. B.; Cram, D. J. *J. Am. Chem. Soc.* **1981**, *103*, 5594.
(10) Helgeson, R. C.; Mazaleyrat, J. P.; Cram, D. J. *J. Am. Chem. Soc.* **1981**, *103*, 3929.

0002-7863/83/1505-4261$01.50/0

Scheme I. The Synthesis of Nickel(II) Complex of Vaulted Macrocyclic Ligands

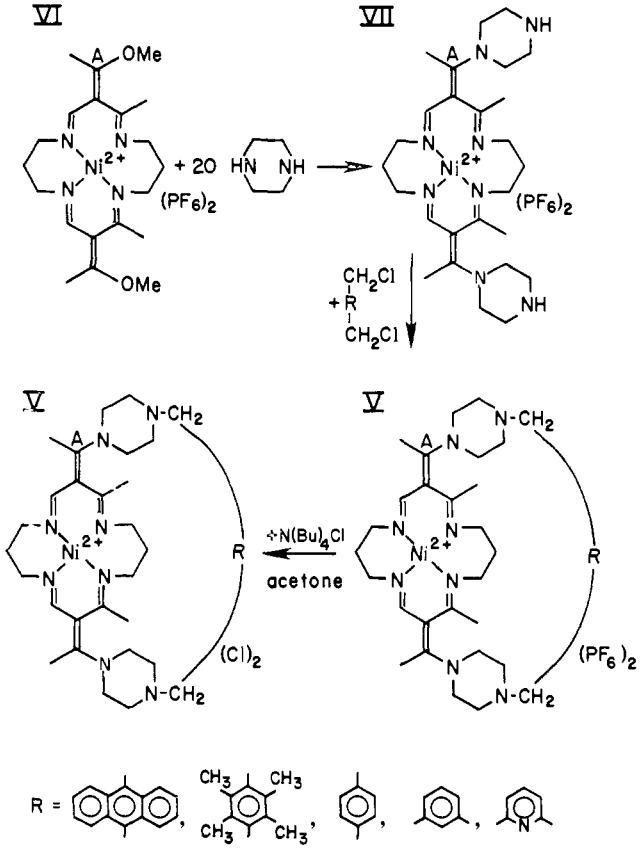

as the basis for design and synthesis of the first examples of metal complexes that can bind both dioxygen and a potential substrate. The result is the vaulted macrobicycle[22] in which the cavity adjacent to one coordination site is greatly expanded (structure V),

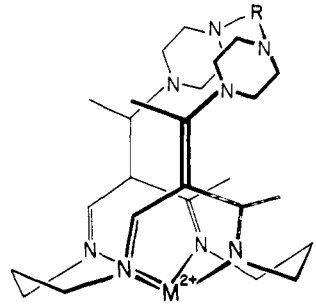

V

Table I. Selected Infrared Absorbances[a] for $[Ni\{R^1(CH_2piperazineEthi)_2Me_2[16]tetraeneN_4\}](X)_2$

R^1, X	ν(C=N,C=C), cm^{-1}	ν(PF), cm^{-1}
9,10-anthracene, PF_6	1608, 1530 (1510)[b]	847, 558
3,6-durene, PF_6	1605, 1540	835, 557
1,4-benzene, PF_6	1610, 1550, 1530	837, 558
1,3-benzene, PF_6	1610, 1545, 1530	832, 557
2,6-pyridine, PF_6	1610, 1535	835, 558
		ν(misc), cm^{-1}
9,10-anthracene, Cl	1600, 1537	(OH, 3320), (C=O, 1700)
3,6-durene, Cl	1600, 1532	(OH, 3340)
1,4-benzene, Cl	1607, 1592, 1542	(OH, 3400), (C=O, 1702)
1,3-benzene, Cl	1600, 1522	(OH, 3300), (C=O, 1707)

[a] Nujol mulls, referenced with polystyrene. [b] C=C stretch of ^{13}C-enriched compound.

while the parent macrocycle, and therefore the ligand field, of structures II and III is retained. Thus, the dioxygen-binding capability should be observed in the cobalt(II) and iron(II) complexes of the vaulted ligands. The ligands have been synthesized as their nickel(II) complexes and characterized by the usual physical and chemical measurements. In addition insight into conformational relationships is obtained by carbon-13 NMR and X-ray structure studies for solution and solid state, respectively. Demonstration of guest–host complexation in aqueous solution is presented in a future paper.

Results and Discussion

The Design and Synthesis of Nickel(II) Complexes of Vaulted Macrobicyclic Ligands. In order to establish a large, potentially commodious void suitable for guest–host association with small organic guest molecules, a large organic superstructure was synthesized onto the 16-membered macrobicyclic ligand structure of the well-investigated family of nickel(II) lacunar compounds.[23-25] The synthesis, diagrammed in Scheme I, involved the appending of piperazine groups onto $[Ni\{(MeOEthi)_2Me_2[16]tetraeneN_4\}](PF_6)_2$, compound VI, yielding $[Ni\{(piperazineEthi)_2Me_2[16]tetraeneN_4\}](PF_6)_2$, compound VII. This compound was then combined with a variety of bis(chloromethyl) aromatic groups to yield compound V, where the Ni-4N plane of the macrocycle forms the floor of a large vaulted region, defined also by the arch of the concatenated grouping: piperazine–aromatic group–piperazine.

The compounds were first isolated and characterized as hexafluorophosphate salts whose solubilities are most appropriate for studies in acetonitrile solution. Water-soluble salts are required for the investigation of guest–host complexing for which the ligands were designed. This was achieved by metathesis to the chloride salts. The metathesis was executed by first dissolving the bis(hexafluorophosphate) salt in acetone and then adding an acetone solution of tetrabutylammonium chloride, resulting in the precipitation of a dichloride salt. The resulting nickel(II) vaulted macrobicyclic dichloride salts exhibit solubilities approaching 0.1 M in water and display NMR spectra indicative of diamagnetic nickel(II) compounds.

An ion-exchange experiment supports the electrolyte type assumed for the nickel(II) complexes of the vaulted macrobicyclic ligands. The chloride salts of the nickel(II) compounds were added to a CM-Sephadex column, and, in all cases, 0.2 M Na_2SO_4

(11) Murakami, Y.; Nakano, A.; Miyato, R.; Matsuda, Y. *J. Chem. Soc., Perkin Trans. 1* **1979**, 1669.
(12) Tabushi, I.; Kuroda, Y.; Kimura, Y. *Tetrahedron Lett.* **1976**, *37*, 3327.
(13) Itui, A.; Iitaki, Y.; Koga, K. *J. Am. Chem. Soc.* **1980**, *102*, 2504.
(14) White, R. E.; Coon, M. J. *Annu. Rev. Biochem.* **1980**, *49*, 315.
(15) White, R. E.; Oprian, D. D.; Coon, M. J. "Microsomes, Drug Oxidations and Chemical Carcinogenesis"; Coon, M. J., Connery, A. H., Estabrook, R. W., Gelboin, H., Gillette, J. R., O'Brien, P. J., Eds.; Academic Press: New York, 1980; p 243.
(16) Herron, N.; Busch, D. H. *J. Am. Chem. Soc.* **1981**, *103*, 1236.
(17) Herron, N.; Cameron, J. H.; Neer, G. L.; Busch, D. H., submitted for publication.
(18) Cameron, J. H.; Kojima, M.; Korybut-Dazkiewicz, B.; Jackson, P. J.; Chavan, M.; Busch, D. H., submitted for publication.
(19) Stevens, J. C.; Jackson, P. J.; Schammel, W. P.; Christoph, G. G.; Busch, D. H. *J. Am. Chem. Soc.* **1980**, *102*, 3283.
(20) Stevens, J. C.; Busch, D. H. *J. Am. Chem. Soc.* **1980**, *102*, 3285.
(21) Kojima, M.; Stevens, J. C.; Jackson, P. J.; Herron, N.; Busch, D. H., in preparation.
(22) Takeuchi, K. J.; Alcock, N.; Busch, D. H. *J. Am. Chem. Soc.* **1981**, *103*, 2421.
(23) Schammel, W. P.; Mertes, K. S. B.; Christoph, G. G.; Busch, D. H. *J. Am. Chem. Soc.* **1979**, *101*, 1622.
(24) Busch, D. H.; Olszanski, D. J.; Stevens, J. C.; Schammel, W. P.; Kojima, M.; Zimmer, L. L.; Holter, K. A.; Mocak, J. *J. Am. Chem. Soc.* **1981**, *103*, 1472.
(25) Busch, D. H.; Jackels, S. C.; Callahan, R. W.; Gryzbowski, J. J.; Zimmer, L. L.; Kojima, M.; Olszanski, D. J.; Mertes, K. S. B.; Christoph, G. G.; Schammel, W. P.; Stevens, J. C.; Holter, K. A.; Mocak, J. *Inorg. Chem.* **1981**, *20*, 2834.

Table II. Proton NMR Data[a] for [Ni{R^1(CH_2piperazineEthi)$_2$$Me_2$[16]tetraene$N_4$}]$(PF_6)_2$

R^1	methyl (N, O)	vinyl (C)	benzylic,[b] (K)	aromatic
9,10-anthracene	2.23, 1.63	7.23	4.86	8.46,[c] 7.53[c]
3,6-durene	2.33, 2.28, 1.86	7.66	3.93	
1,4-benzene	2.36, 1.80	7.26	3.80	7.43[d]
1,3-benzene	2.40, 1.83	7.43	3.88	7.26[d]
2,6-pyridine	2.40, 1.83	7.43	4.10	7.75,[e] 7.30[f]

[a] Spectra recorded in CD_3CN with chemical shifts (δ) referenced from Me_4Si. [b] Chemical shifts listed are the center of an AB quartet. [c] Complex multiplet. [d] Broad multiplet. [e] Triplet multiplet. [f] Doublet multiplet.

aqueous solution was sufficient to elute the nickel(II) complex. Earlier studies[25] with very similar complexes support the conclusion that the nickel(II) complexes must therefore be present as dipositive ions and not as dimers or other oligomers.

Characterization of the Nickel(II) Complexes of the Vaulted Macrobicyclic Ligands. The nickel(II) vaulted compounds were characterized through elemental analysis and infrared, proton, and carbon-13 spectroscopic studies.

The compounds from Scheme I are readily monitored by infrared spectroscopy (Table I). For the case of [Ni{9,10-anthracene(CH_2piperazineEthi)$_2$$Me_2$[16]tetraene$N_4$}]$(PF_6)_2$, the spectrum of compound VI possesses peaks due to the imine groups (1632 cm^{-1}) conjugated with a symmetrically substituted alkene moiety (1580 cm^{-1}). In addition, the two intense peaks at 1283 and 1028 cm^{-1} are indicative of the presence of an alkene-substituted ether, while the peaks at 836 and 670 cm^{-1} are characteristic of the presence of a hexafluorophosphate anion. The spectrum of compound VII possesses a peak at 1608 cm^{-1} showing the retention of the imine groups, in conjugation with an alkene group (1526 cm^{-1}) and the retention of the hexafluorophosphate anion (832 and 560 cm^{-1}). However, the alkene-substituted ether peaks are absent and a weak N–H stretch is present at 3335 cm^{-1}, as required when piperazine replaces methoxide and forms a secondary amine. Compound V retains the peaks for imine groups (1608 cm^{-1}) in conjugation with an alkene group (1530 cm^{-1}) and the peaks for the hexafluorophosphate anion (837 and 558 cm^{-1}); however, the secondary amine N–H stretch vanishes and a sharp peak appears at 769 cm^{-1}, indicative of the presence of the anthracene group (out-of-plane C–H bend). The presence of acetonitrile is indicated by the band at 2244 cm^{-1}. In addition to the bands mentioned, all nickel(II) vaulted compounds possess a distinctive fingerprint pattern in the 900–1300 cm^{-1} range.

Finally, the spectrum of the chloride salt of compound V retains the characteristic absorptions for alkene and imine groups (1537, 1600 cm^{-1}). However, the bands due to the hexafluorophosphate anion are absent. In addition, the spectra of the chloride salts generally possess a broad peak in the 3300–3400 cm^{-1} range, due to water of crystallization, and a sharp band in the 1700–1707 cm^{-1} range, due to acetone of crystallization. The presence of these solvent molecules is corroborated by elemental analysis.

The proton NMR spectra for the nickel(II) derivatives of the vaulted macrobicyclic ligands are summarized in Table II. The proton NMR spectrum of [Ni{9,10-anthracene(CH_2piperazineEthi)$_2$$Me_2$[16]tetraene$N_4$}]$(PF_6)_2$ (Figure 1) is exemplary. Several features of this proton NMR spectrum are typical of all of these compounds. First, all of the compounds possess mirror symmetry. Second, all display two single resonances, labeled N and O, in the range 1.63–2.40 ppm, corresponding to the two methyl groups of the parent macrobicycle. Third, all possess a singlet, labeled C, in the range between 7.23 and 7.66 ppm, which corresponds to the vinyl proton of the parent macrocycle. Finally, all nickel(II) vaulted compounds display an AB quartet pattern in the range from 3.80 to 4.86 ppm; this arises from the two benzylic protons of the superstructure arch. The specific values of the resonances labeled C, K, N, and O for [Ni{9,10-anthracene(CH_2piperazineEthi)$_2$$Me_2$[16]tetraene$N_4$}]$(PF_6)_2$ are listed in Table II. The multiplets labeled RR′ and SS′ in Figure 1 (8.46 and 7.53 ppm) correspond to the inner (RR′) and outer (SS′) protons, respectively, of the anthracene rings. All other protons correspond to the several methylene groups and their resonances appear as broad multiplets in the range from 1.5 to 4.0 ppm. The integrations of the various peaks agree with the above assignments.

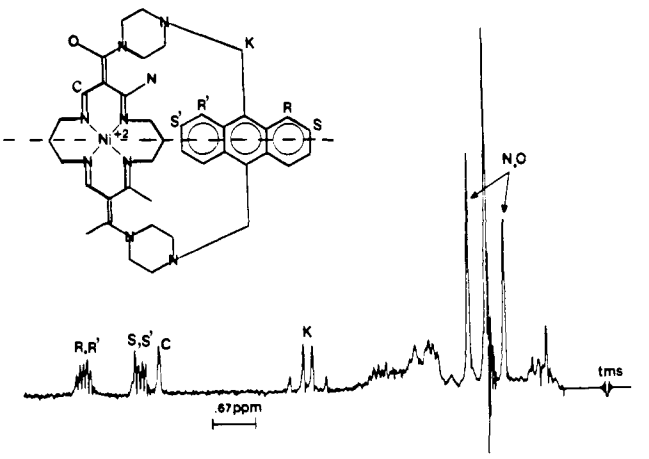

Figure 1. Proton NMR spectrum of [Ni{9,10-anthracene(CH_2piperazineEthi)$_2$$Me_2$[16]tetrazene$N_4$}]$(PF_6)_2$.

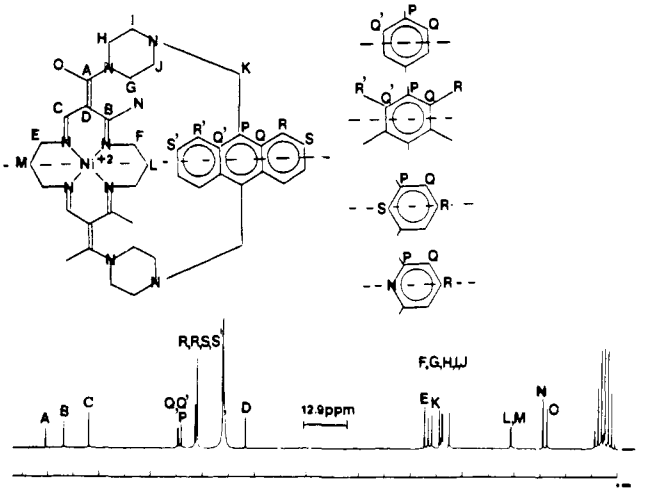

Figure 2. Carbon-13 NMR spectrum of [Ni{9,10-anthracene(CH_2piperazineEthi)$_2$$Me_2$[16]tetraene$N_4$}]$(PF_6)_2$.

Carbon-13 NMR studies played a large role in both the characterization of the nickel(II) complexes of the vaulted macrobicyclic ligands and in the determination of their conformations in solution. Several features of the carbon-13 NMR spectrum of [Ni{9,10-anthracene(CH_2piperazineEthi)$_2$$Me_2$[16]tetraene$N_4$}]$(PF_6)_2$ (Figure 2) are typical of those of all of the nickel(II) vaulted compounds (Table III).[26] As with the proton NMR spectra, the mirror symmetry is evident in the carbon-13 NMR results. From chemical shift and off-resonance measurements, the carbon-13 NMR spectra of nickel(II) vaulted compounds can be divided into discrete regions. Three peaks occur in the range 174.2–159.3 ppm; these can be assigned to the resonances of carbon atoms A, B, and C (Figure 2), all of which are imine-type carbon atoms. With use of off-resonance decoupling techniques, the two bands furthest downfield remain singlets and can be assigned to carbon atoms A and B. The third peak splits into a doublet, indicating coupling to a single proton and leading to the assignment of the band to carbon atom C. The peak associated with carbon atom D, a totally substituted alkene carbon atom, is found in the range from 111.8 to 111.0 ppm; it remains a singlet upon off-resonance decoupling. Resonances corresponding to the seven different methylene carbons that are bonded to nitrogen atoms (E, F, G, H, I, J, K) all occur in the range 64.5–48.4 ppm.

(26) Many of the assignments are based on earlier studies.[24]

Table III. Carbon-13 NMR Data[a] for $[Ni\{R^1(CH_2piperazineEthi)_2Me_2[16]tetraeneN_4\}](PF_6)_2$

R^1	chemical shifts[b]
9,10-anthracene	A, 173.0; B, 167.3; C, 159.6; D, 111.5; E, 56.7; F, G, H, I, J, 55.5, 54.4, 51.4, 51.0, 49.1; K, 52.1; L, M, 30.3, 30.1; N, 20.3; O, 19.1; P, 131.1; Q, Q', 132.2, 131.8; R, R', 126.8, 126.1; S, S', 126.3, 126.1
3,6-durene	A, 174.2; B, 167.6; C, 159.3; D, 111.8; E, F, G, H, I, J, K, 56.6, 56.3, 54.3, 53.7, 51.4, 51.0, 48.4, L, M, 30.4, 30.2; N, 20.0; O, 19.1; P, Q, Q', 135.5, 134.9, 134.4; R, R', 17.5, 16.8
1,4-benzene	A, 171.4; B, 167.8; C, 160.3; D, 111.0; E, F, G, H, I, J, K, 61.4, 56.6, 55.7, 54.6, 51.4, 50.3; L, M, 30.6, 30.0; N, 21.0; O, 19.0; P, 137.9; Q, Q'', 131.0
1,3-benzene	A, 172.4; B, 168.1; C, 160.0; D, 111.7; E, F, G, H, I, J, K, 62.2, 56.7, 55.7, 55.0, 51.5, 50.5; L, M, 30.4; N, 20.5; O, 18.7; P, 137.9; Q, 129.6; R, S, 135.0, 130.0
2,6-pyridine	A, 171.9; B, 167.8; C, 160.0; D, 111.5; E, F, G, H, I, J, K, 64.5, 56.7, 55.8, 55.4, 52.3, 51.6, 50.4; L, M, 30.3; N, 20.4; O, 18.7; P, 156.9; Q, 124.2; R, 138.9

[a] CD_3CN solution, ppm relative to $NCCD_3$ (118.2 ppm). [b] Labeling scheme from Figure 2.

Figure 3. Effect of 90% carbon-13 NMR enrichment on the carbon-13 NMR spectrum of $[Ni\{9,10\text{-anthracene}(CH_2piperazineEthi)_2Me_2[16]tetraeneN_4\}](PF_6)_2$.

In off-resonance experiments, all seven peaks split into triplets, indicative of the two protons bonded to each carbon atom. The two bands occurring in the range from 30.6 to 30.0 ppm can be assigned to carbon atoms L and M, which are methylene carbon atoms two bonds removed from a nitrogen atom. Again, off-resonance experiments cause peaks to split into triplets. The resonances of methyl carbon atoms bonded to imine carbons occur as separate bands in the range from 21.0 to 18.8 ppm. As required, each peak splits into a quartet upon off-resonance decoupling.

The unique absorptions in the carbon-13 NMR spectra of the individual nickel(II) vaulted compounds are due to the specific R^1 groups contained in the superstructure arch (Scheme I). For R^1 = 9,10-anthracene, seven peaks are present in the range from 132.2 to 126.1 ppm; these correspond to carbon atoms P, Q, Q', R, R', S, and S' (Figure 2). With use of off-resonance techniques, the three peaks at 131.1, 131.8, and 132.2 ppm remain singlets and can be assigned to carbon atoms P, Q, and Q', all substituted aromatic carbon atoms. The remaining peaks split into doublets, indicating that a single proton is bonded to each carbon atom and these are R, R', S, and S' (Figure 2). For R^1 = 3,6-durene, three peaks at 134.4, 134.9, and 135.5 ppm can be assigned to carbons P, Q, and Q' (Figure 2). In addition the two peaks at 17.5 and 16.8 ppm can be assigned to carbon atoms R and R'. As expected the three peaks corresponding to carbon atoms P, Q, and Q' remained singlets (substituted aromatic carbon atoms) while the two peaks assigned to the methyl carbon atoms R and R' split into quartets upon off-resonance decoupling.

For R^1 = 1,4-benzene, only two peaks are attributable to the benzene moiety (137.9 and 131.0 ppm). The band at 137.9 ppm has been assigned to carbon atom P, a substituted aromatic carbon atom, while the peak at 131.0 ppm is assigned to both carbon atoms Q and Q', on the basis of off-resonance experiments. This implies that carbon atoms Q and Q' are equivalent on the NMR time scale at ambient temperature (30 °C) with acetonitrile-d_3 as the solvent. Since only carbon atoms Q and Q' appear equivalent in the carbon-13 NMR spectrum of $[Ni\{1,4\text{-benzene}(CH_2piperazineEthi)_2Me_2[16]tetraeneN_4\}](PF_6)_2$, their fluxionality must occur primarily through rapid rotation about the KP bonds.

For R^1 = 1,3-benzene, four peaks are assignable to the benzene group (137.9, 135.0, 130.3, and 129.6 ppm). Again, on the basis of off-resonance studies, the peak at 137.9 ppm (singlet) can be assigned to carbon atom P, while the remaining three peaks all split into doublets. Since there are two carbon atoms Q for each carbon atom R and each carbon atom S, the peak at 129.6 ppm, which is roughly twice the height of the other two, can be assigned to carbon atom Q. The carbon-13 NMR spectrum for R^1 = 2,6-pyridine can be interpreted similarly to that of R^1 = 1,3-benzene spectrum, with the peak at 156.9 ppm assigned to carbon atom P, the peak at 138.9 ppm, to carbon atom P, and the peak at 124.2 ppm, to carbon atom Q.

Through 90% carbon-13 enrichment of carbon atom A (Figure 3) in the compounds $[Ni\{(piperazineEthi^*)_2Me_2[16]tetraeneN_4\}](PF_6)_2$, $[Ni\{9,10\text{-anthracene}(CH_2piperazineEthi^*)_2Me_2[16]tetraeneN_4\}](PF_6)_2$, and $[Ni\{1,4\text{-benzene}(CH_2piperazineEthi^*)_2Me_2[16]tetraeneN_4\}](PF_6)_2$, resonances for carbon atoms A, B, N, and O (Figures 2 and 3) of the macrobicycle have been unequivocally assigned to their respective carbon-13 NMR peaks. This has removed many of the ambiguities in the assignments of the resonances for these compounds. The carbon-13 NMR spectrum of $[Ni\{9,10\text{-anthracene}(CH_2piperazineEthi^*)_2Me_2[16]tetraeneN_4\}](PF_6)_2$ (Figure 3) shows that carbon-13 enrichment at carbon atom A dramatically increases the intensity of the peak farthest downfield, requiring assignment of that resonance to carbon atom A, (range for all compounds 174.2–171.4 ppm). Since the resonance for carbon atom B is very similar to the resonance for carbon A in terms of chemical shift and off-resonance decoupling behavior, the adjacent peak in the range from 168.1 to 167.3 ppm is assigned to carbon atom B. In addition, the peak for carbon atom O should split into a doublet upon carbon-13 enrichment at atom A. Indeed, the peak furthest upfield (range from 19.1 to 18.7 ppm) does split into a doublet. Since the absorption for carbon atom N is very similar to the one for carbon atom O (chemical shift and off-resonance decoupling), the feature in the range from 21.0 to 20.0 ppm can be assigned as the resonance for carbon N.

The carbon-13 NMR spectrum of $[Ni\{9,10\text{-anthracene}(CH_2piperazineEthi)_2Me_2[16]tetraeneN_4\}](PF_6)_2$ shows (Figure 4) that the resonance of carbon atom C is split into a doublet of triplets upon gated decoupling. The doublet is the result of the coupling of C with the proton directly bonded to it while the smaller triplets are due to the coupling of carbon atom C with, most probably, the two protons of carbon atoms E—three bonds distant from

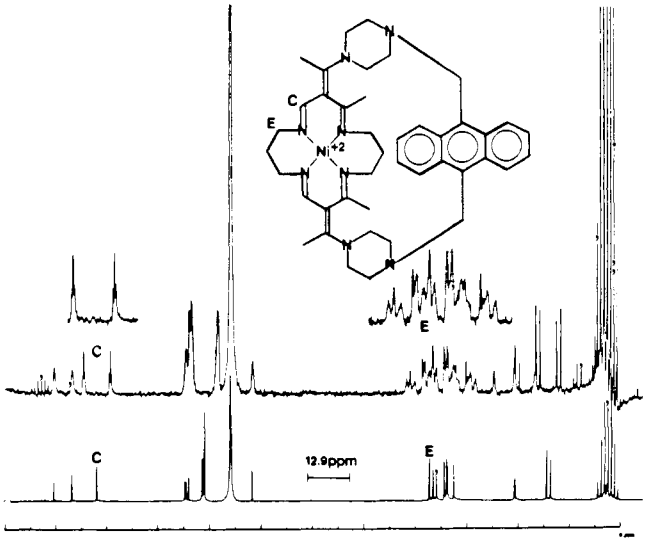

Figure 4. Proton coupling effects on the carbon-13 NMR spectrum of [Ni{9,10-anthracene(CH_2piperazineEthi)$_2$$Me_2$[16]tetraene$N_4$}]($PF_6$)$_2$.

carbon atom C. A similar relationship holds for carbon atom E (Figure 4). One of the seven peaks (52.1 ppm) in the range from 56.7 to 49.1 ppm splits into a triplet of doublets. The remaining six peaks split into triplets. This suggests that the proton bound to carbon atom C couples in a similar three bond relationship to carbon atom E.

X-ray Crystal Structure Determination of [Ni{9,10-anthracene(CH_2piperazineEthi)$_2$[16]tetraeneN_4}](PF_6)$_2$·2CH_3CN. A major objective of the design and synthesis of the vaulted macrobicyclic ligands and their complexes is the generation of a nickel(II) macrobicyclic compound retaining the basic structural characteristics of the lacunar family of compounds and also possessing a large commodius void. The results of the X-ray crystal structure determination verify that the compounds reported here fulfill this objective.

As shown in Figures 5 and 6, [Ni{9,10-anthracene(CH_2-piperazineEthi)$_2$$Me_2$[16]tetraene$N_4$}]($PF_6$)$_2$·2$CH_3CN$ retains the basic structural characteristics of the lacunar family of macrobicyclic compounds. N1, N2, N3, and N4 are in a square-planar arrangement, and all four Ni–N distances are within 0.01 Å of 1.89 Å and all four N-Ni-N angles are within 2° of 90°. Second, the macrocycle assumes a saddle conformation where the two saturated trimethylene chelate rings are on one side of the Ni–4N plane (below the void), while the two unsaturated, substituted chelate rings project upward on the opposite side of the Ni–4N plane and constitute parts of the sidewalls of the vaulted void. In addition, the six-membered saturated chelate ring comprised of atoms Ni, N1, C1, C2, C3, and N2 has a chair conformation while the six-membered saturated chelate ring comprised of atoms Ni, N3, C7, C8, C9, and N4 has a boat conformation. Third, atoms Ni, N1, N2, N3, N4, C5, C6, C10, C11, C16, and C42 are all coplanar with respect to their nearest neighbors. Finally, there are no chemically unusual angles or bond distances present in the structure of the parent macrocyclic components, as diagramed in Figure 6. The uncertainties in the bond lengths listed in Figure 6 are approximately ±0.01 Å, and that for the bond angles is approximately ±0.1°.

The superstructure of compound V (R = 9,10-anthracene) is displayed in Figure 5,where the two piperazine rings, in chair conformation, rise above the Ni–4N plane and bond at the 9,10-positions to an anthracene moiety. The conformational rigidities of the piperazine rings and the anthracene groups maintain, in the solid state, a large void adjacent to one of the unused axial coordination positions of the nickel atom. This truncated pyramidal void can be described by several key distances and angles. The dimensions of the larger opening of the pyramidal void are 8.24 Å from the midpoint of the N1N2 line to the midpoint of the C30C35 line by 8.95 Å from atom C15 to atom C42. The smaller opening of the void closes to 7.26 Å from the midpoint of the N3N4 line to the midpoint of the C23C28 line by 6.57 Å from atom N5 to atom N8. The plane of the anthracene group is tilted 30.9° from the parallel with respect to the Ni–4N plane.

The crystal structure affirms the analyses of the spectroscopic results gathered for the nickel(II) vaulted macrocyclic compounds. The presence of conjugated alkene and imine functionalities suggested by the infrared spectroscopic data is confirmed by the two conjugated alkene–imine systems generated by planar atoms N1, N4, C10, C11, C12, and C42 and by planar atoms N2, N3, N4, C5, and C6 (Figures 5 and 6). The short C–N (1.34 Å) and C–C (1.42 Å) bond distances involved in these two alkene–imine systems reinforce the concept of a conjugated alkene–imine bonding scheme. However, the torsion angles between planar atoms N4 and C10 of 11.8°, between planar atoms C10 and C11 of 28.4°, and between planar atoms C11 and C41 of 38.6° indicate that the planar atoms N4, C10, C11, and C41 are not mutually coplanar and any arguments involving total π overlap of the conjugated alkene–imine system are not appropriate. Upon examination of Figure 5, a mirror plane, as required by the NMR results, can be envisioned as containing carbon atoms C2 and C8, the nickel atom, and the midpoints of the C23C28 line and of the C30C35 line, although no crystallographic mirror is present. In addition, all proton and carbon atom types suggested by NMR spectroscopy are confirmed. Finally, the compound under examination is a monomeric 2:1 electrolyte, as predicted by the ion-exchange data.

An interesting and important feature of the crystal structure is the presence of two acetonitrile molecules, an "external" ace-

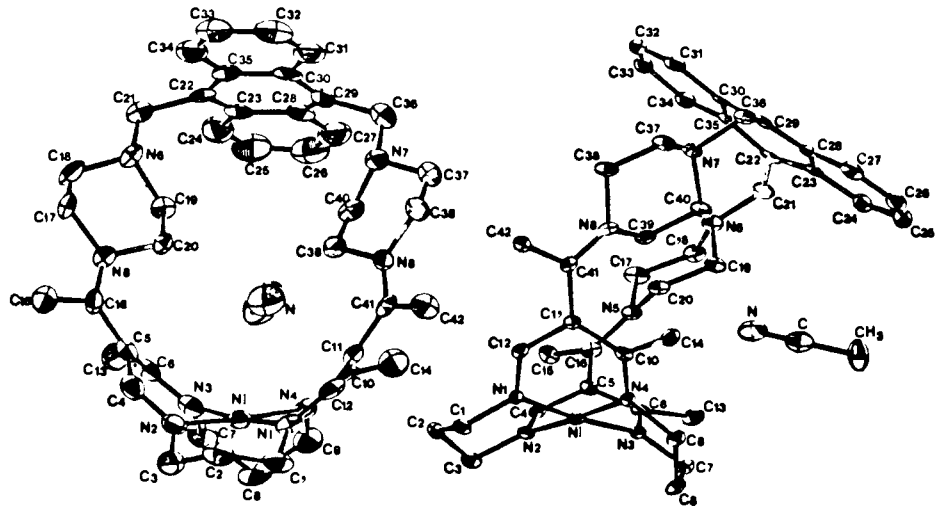

Figure 5. ORTEP diagrams and numbering scheme of [Ni{9,10-anthracene(CH_2piperazineEthi)$_2$$Me_2$[16]tetraene$N_4$}]($PF_6$)$_2$.

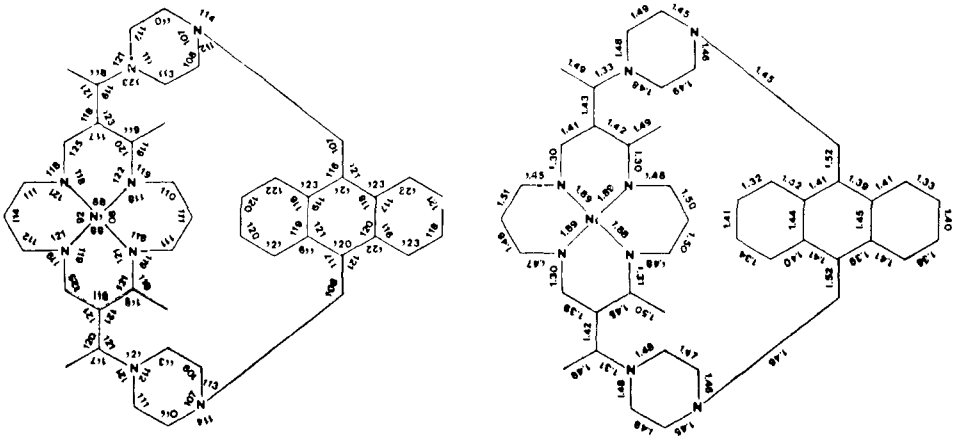

Figure 6. Bond lengths and bond angles for [Ni{9,10-anthracene(CH_2piperazineEthi)$_2$$Me_2$[16]tetraeneN$_4$}]$(PF_6)_2$·2$CH_3CN$.

tonitrile, present as solvent of crystallization, and an "internal" actonitrile, present partially within the confines of the void that is formed by the chelating macrocycle and the appended superstructure (Figure 5). Considering the plane described by carbon atoms C25, C26, and C8 as defining the limits of the cavity, the "internal" acetonitrile molecule is mostly within the vaulted region. A most striking aspect of the acetonitrile solvate of the vaulted nickel(II) complex involves the mode of association between the nitrogen atom (IN) of the acetonitrile and six protons of the macrobicyclic ligand. As shown in Figure 7, the internuclear distances between the acetonitrile nitrogen atom and the protons from carbon atoms C7, C9, C18, C19, C39, and C40 all fall within 0.05 Å of 2.91 Å, the van der Waals contact distance[27] between a nitrile nitrogen atom and a hydrogen atom bonded to a methylene carbon atom. Since there are no other significant contacts between the associated acetonitrile and the complex, these six points of van der Waals contact are crucial to this intermolecular guest–host association. This intimate association between guest acetonitrile and host nickel complex has been achieved by an accommodating conformational change by the host species. This is accomplished by a simple pivoting of the piperazine rings about their C16N5, C21N6, C36N7, and C41N8 axes, thus maximizing the van der Waals contacts while retaining the typical spacial conformation of the macrobicyclic structure. No major conformational rearrangements of either the chelating macrocyclic structure or of the piperazine ring (boat–chair conformations) need be employed in this pivoting of the piperazines to accommodate the guest. It must be emphasized that this guest–host behavior typifies such an interaction in a hydrophobic nonpolar environment. In aqueous solutions, the nitrogen atom of the acetonitrile is expected to interact with solvent. This should result in reversing the orientation of any such guest molecule with respect to the host cavity.

Coordinates for the atoms and thermal parameters are given in Table IV. Structure factors are recorded as supplementary material.

The Conformations of the Nickel(II) Vaulted Compounds in Solution. In order to affect guest–host association between small organic molecules (guests) and the nickel(II) vaulted macrobicyclic compounds (hosts), the conformation of the host compounds in the solution phase must maintain the large void present in the solid state. Spectroscopic data on the nickel(II) vaulted macrobicyclic compounds indicate that their conformation is variable and that the potentially commodious void is available in solution.

In general, the major difference between the ambient temperature (30 °C) carbon-13 NMR spectrum of compound VII and that of the vaulted nickel(II) compound is that in the former there are only two peaks corresponding to the piperazine carbon atoms while in the latter there are four peaks. Thus in compound VII, the piperazine carbon atoms G and H and atoms I and J

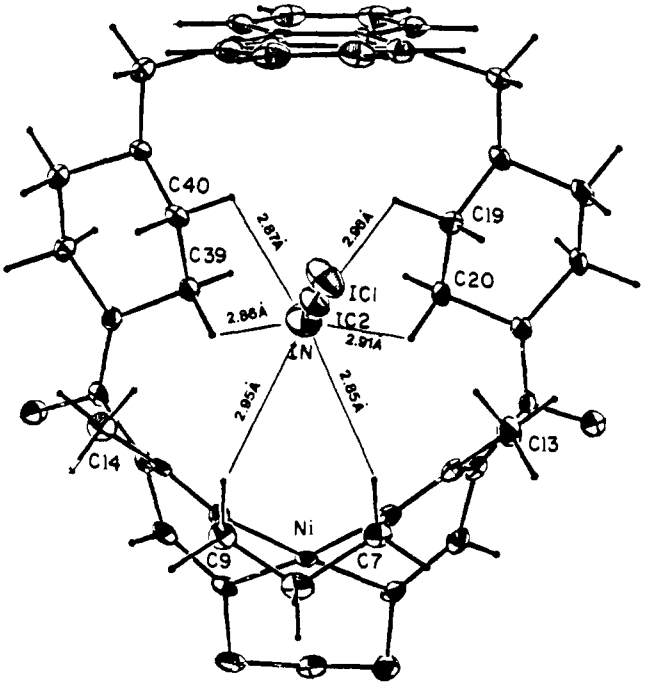

Figure 7. Mode of association between an *internal* acetonitrile and the host molecule.

(Figure 2) are pairwise equivalent on the NMR time scale, while in the nickel(II) vaulted complex all four carbon atoms are unique. A straight forward interpretation of this phenomenon is that in compound VII the piperazine rings rotate rapidly about their nitrogen–carbon axes, causing interconversion of carbon atoms G and H and of carbon atoms I and J. Upon completion of the superstructure arch (compound V) the piperazine rings can no longer rotate rapidly about their nitrogen–carbon axes; this of course causes each of the four piperazine carbon atoms to exhibit its unique spectral band. The crystal structure data reinforce this interpretation, for the piperazine rings cannot rotate fully about their axes without sterically interacting with each other (Figure 5). For example, in the orientation in Figure 5, the hydrogen atoms from carbon atoms 20 and 29 are separated by 2.83 Å, which is already close to the van der Waals contact distance. Further rotation of the piperazines toward each other is obviated.

While completion of the arch; i.e., formation of the vaulted compounds, results in the cessation of rapid piperazine rotation, both the carbon-13 and proton NMR spectra of the specific compound V in which R^1 = 1,4-benzene suggests that the benzene ring participates in fluxional behavior at appropriate temperatures in acetonitrile, acetone, and water solvents. The carbon-13 NMR spectrum, in acetone-d_6, displays two peaks in the aromatic carbon atom region, as shown in Figure 8. On the basis of previously

(27) Kitaigorosky, A. "Molecular Crystals and Molecules"; Academic Press: New York, 1973.

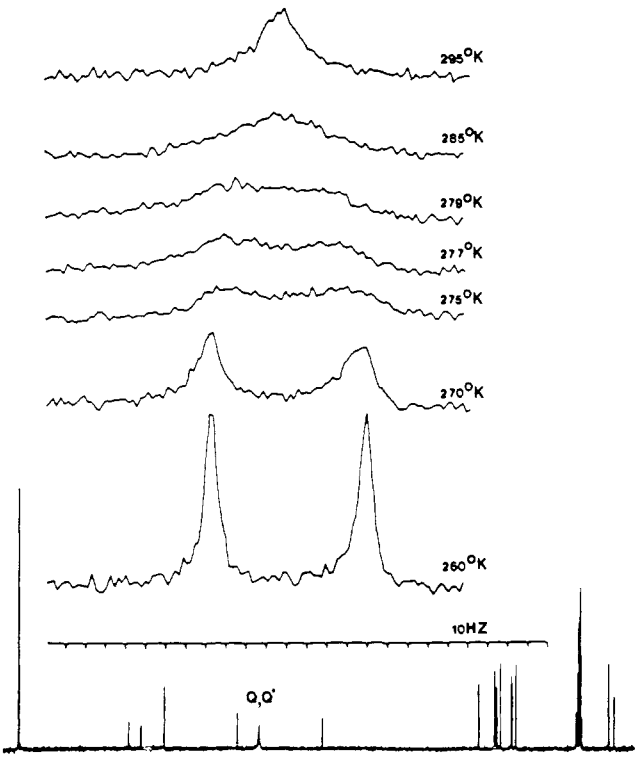

Figure 8. The fluxional behavior as observed in acetone solution by carbon-13 NMR for the 1,4-benzene-bridged vaulted complex.

mentioned off-resonance proton decoupling experiments, the smaller peak is assigned (Table III) to carbon atom P while the larger peak was assigned to the unsubstituted carbon atoms Q and Q′ (Figure 2). When the sample is cooled from 295 to 260 K, the singlet at 131.0 ppm gradually splits into a doublet. The proton NMR spectra of compound V, R^1 = 1,4-benzene with acetonitrile-d_3 or deuterium oxide as the solvent, display two singlets in the 7–8 ppm range, where the upfield peak was assigned to the vinylic proton bonded to carbon atom C, while the downfield peak was assigned to the aromatic protons bonded to carbon atoms Q and Q′ (Table II). When the sample temperature is lowered, the peak assigned to the aromatic protons splits into two peaks.

These observations lead to the conclusion that the benzene ring is undergoing rapid rotation about its carbon atom K–carbon atom P axis at elevated temperatures, causing the interconversion of carbon atoms Q and Q′. The rotation is slowed by lowering the temperature until the atoms that had been averaged by the motion display their individual resonances. A number of examples of this type of fluxional behavior have been reported,[28] many involving rotation about partial double bonds, such as an amide C–N bond.[29]

The relationship between the two specific fluxional behaviors described above is of critical importance in indicating solution structural relationships. From the crystal structure data of compound V where R^1 = 9,10-anthracene, in order for R^1 = 1,4-benzene to rotate about its carbon atom K–carbon atom P axis, the piperazine rings must pivot about their carbon atom A–nitrogen atom and carbon atom K–nitrogen atom axes (Figure 6) such that the distances between carbon atoms 20 and 30 and between carbon atoms 17 and 38 are approximately equal and maximized. If this "parallel" conformation is maintained, then a 1,4-disubstituted benzene in the R^1 position can rotate without steric interference. The evidence relating to the pivoting of the piperazine rings enhances the probability that the nickel(II) vaulted compounds provide a large accommodating void in solution.

The fluxional phenomena described here are general in that both proton and carbon-13 studies were applicable and in that the behavior was observed in acetonitrile-d_3, acetone-d_6, and deuterium oxide. Also, since 9,10-anthracene and 3,6-durene differ from 1,4-benzene only in the substitutents on the central six-membered, aromatic, para-substituted ring, it is anticipated that the pivoting of the piperazine rings deduced for compound V where R^1 = 1,4-benzene is highly probable for the other compounds V as well, even though their R^1 groups are too bulky to spin.

To reinforce the similarities of the macrocyclic structures in compounds VII and V (Scheme I), it should be noted that the infrared frequencies for the imine and alkene stretching modes do not vary by more than 10 cm^{-1} from compound VII values (1610, 1530 cm^{-1}) to compound V values (Table I). Thus, upon reaction of compound VII with an R^1 group to yield the corresponding compound V, no major macrocyclic structural changes appear to accompany the cessation of the piperazine rotation. Other studies have shown that the half-wave potential of the electrochemical Ni^{2+}/Ni^{3+} couple is unaffected by inhibiting or liberating this rotational motion.

Further, the carbon-13 NMR coupling constants $^1J_{AC}$ and $^1J_{AO}$ for 90% enriched carbon atom A in labeled compounds VII and V (R^1 = 9,10-anthracene; 1,4-benzene) are identical with $^1J_{AC}$ = 71.3 Hz and $^1J_{AO}$ = 43.9 Hz in both cases (Figure 3). Since the coupling constants are sensitive to both s charcter of the bond between coupled carbon atoms and the electronegativities of their substituents,[30] there appears to be little disturbance of the macrocyclic structure upon reaction of compound VII to form compound V, even though piperazine ring rotation has been greatly restricted.

It should be noted that the $^1J_{AO}$ value of 43.95 Hz is in good agreement with that found for coupling between the sp^3 carbon atom and the sp^2 carbon atom in toluene (44 Hz), while the $^1J_{AC}$ value of 71.3 Hz agrees well with typical values of ~70 Hz for coupling between pairs of sp^2 carbon atoms in alkenes.[31] The crystal structure data support these inferred hybridizations and indicate that there is no major change in hybridization in going from the solid state to solution.

Experimental Section

Reagents and Solvents. All reagents, solvents and chemicals were reagent grade and used without further purification unless otherwise stated.

Synthesis of Unbridged Nickel(II) Complexes. (3,11-Diacetyl-4,10-dimethyl-1,5,9,13-tetraazacyclohexadeca-1,3,9,11-tetraenatoN$_4$)nickel-(II), [Ni(Ac$_2$Me$_2$[16]tetraenatoN$_4$)]. This complex was synthesized according to a published procedure.[32]

(2,12-Dimethyl-3,11-bis[1-methoxyethylidene]-1,5,9,13-tetraazacyclohexadeca-1,4,9,12-tetraeneN$_4$)nickel(II) Hexafluorophosphate, [Ni{(MeOEthi)$_2$Me$_2$[16]tetraeneN$_4$}](PF$_6$)$_2$. This complex was synthesized according to the procedure of Schammel.[33]

(2,12-Dimethyl-3,11-bis[1-(1-piperazinyl)ethylidene]-1,5,9,13-tetraazacyclohexadeca-1,4,9,12-tetraeneN$_4$)nickel(II) Hexafluorophosphate, [Ni{(piperazineEthi)$_2$Me$_2$[16]tetraeneN$_4$}](PF$_6$)$_2$. A solutuion of 3.54 g (5 mmol) of [Ni{(MeOEthi)$_2$Me$_2$[16]tetraeneN$_4$}](PF$_6$)$_2$ dissolved in 100 mL of acetonitrile was slowly added to a solution of 8.61 g (0.1 mol) of piperazine dissolved in 100 mL of methanol. The resulting orange solution was reduced in volume, inducing an orange crystalline precipitate. This precipitate was recrystallized from an acetonitrile/methanol (1:2 v/v) solution; yield 1.2 g (29.2%). Anal. Calcd for $NiC_{30}H_{48}N_8P_2F_{12}$: C, 38.21; H, 5.43; N, 13.71. Found: C, 38.14; H, 5.58; N, 13.65.

Synthesis of Bridged Nickel(II) Compounds. (2,17,19,25-Tetramethyl-3,6,13,16,20,24,27,31-octaazapentacyclo[16.7.7.2^{8,11}.2^{3,6}.2^{13,16}]-hexatetraconta-1,8,10,17,19,24,26,31,33-nonaeneN$_4$)nickel(II) Hexafluorophosphate, [Ni{1,4-benzene(CH$_2$piperazineEthi)$_2$Me$_2$[16]tetraeneN$_4$}](PF$_6$)$_2$. One gram (1.2 mmol) of [Ni{(piperazineEthi)$_2$Me$_2$[16]tetraeneN$_4$}](PF$_6$)$_2$ was dissolved in 100 mL of acetonitrile; 0.35 g (1.3 mmol) of *p*-bis(chloromethyl)benzene was dissolved in 100 mL of acetonitrile, and both solutions were dipped simultaneously into a res-

(28) "Dynamic NMR Spectroscopy"; Jackman, L., Cotton, F. Eds.; Academic Press: New York, 1975.

(29) For example, the rotation about the C–N bond in *N,N*-dimethylformamide (Bovey, F. *Chem. Eng. News* **1965**, *43*, 98).

(30) Wasylishen, R. "Annual Reports on NMR Spectroscopy"; Webb, G., Ed.; Academic Press: London, 1977; p 249.

(31) Stothers, J. "Carbon-13 NMR Spectroscopy"; Academic Press: New York, 1972.

(32) Riley, D. P.; Busch, D. H. *Inorg. Synth.* **1978**, *18*, 36.

(33) Schammel, W. P.; Zimmer, L. L.; Busch, D. H. *Inorg. Chem.* **1980**, *19*, 3159.

(34) Obtained from Prochem-Isotopes, Summit, NJ.

Table IV. Atomic Positions and Temperature Factors for [Ni{9,10-anthracene(CH_2piperazineEthi)$_2$$Me_2$[16]tetraeneN$_4$}]($PF_6$)$_2$·2$CH_3CN$[a]

atom	x	y	z	U(11)	U(22)	U(33)	U(12)	U(13)	U(23)
Ni	0.4081 (8)	0.53352 (6)	0.32638 (4)	3.48 (7)	4.00 (6)	3.91 (6)	0.18 (6)	1.47 (5)	0.37 (5)
N1	0.5717 (5)	0.6151 (3)	0.3779 (3)	4.2 (4)	3.5 (4)	4.7 (4)	−0.0 (3)	1.6 (3)	−0.3 (3)
N2	0.3634 (5)	0.6040 (4)	0.2613 (3)	3.9 (4)	5.4 (4)	4.4 (4)	0.7 (4)	1.0 (3)	1.0 (3)
N3	0.3577 (5)	0.4495 (4)	0.2735 (3)	3.3 (4)	4.6 (4)	5.0 (4)	−0.3 (3)	0.6 (3)	0.4 (3)
N4	0.4599 (5)	0.4606 (4)	0.3889 (2)	4.5 (4)	4.3 (4)	4.0 (3)	0.0 (3)	1.5 (3)	0.8 (3)
N5	0.5140 (5)	0.4486 (4)	0.1372 (3)	4.5 (4)	7.1 (5)	3.2 (3)	0.7 (4)	0.8 (3)	0.0 (3)
N6	0.6585 (5)	0.3291 (4)	0.1316 (3)	5.2 (5)	8.0 (5)	2.9 (3)	0.4 (4)	1.5 (3)	0.1 (3)
N7	0.8833 (5)	0.3497 (4)	0.3791 (3)	4.4 (4)	6.6 (5)	4.3 (4)	0.9 (4)	0.8 (3)	−1.3 (3)
N8	0.7708 (5)	0.4724 (4)	0.4187 (2)	3.5 (4)	6.6 (5)	3.3 (3)	−0.0 (4)	0.8 (3)	0.5 (3)
C1	0.4260 (7)	0.6920 (5)	0.3790 (4)	4.8 (6)	5.0 (6)	6.0 (6)	0.7 (5)	1.7 (5)	−1.1 (5)
C2	0.3984 (7)	0.7288 (5)	0.3169 (4)	4.7 (6)	4.6 (5)	7.2 (7)	0.7 (5)	1.9 (5)	0.2 (5)
C3	0.3256 (7)	0.6828 (5)	0.2714 (4)	5.0 (6)	4.8 (6)	5.4 (6)	1.6 (5)	1.4 (5)	0.6 (5)
C4	0.3786 (6)	0.5868 (5)	0.2084 (3)	4.0 (5)	4.8 (6)	4.1 (5)	0.1 (5)	0.8 (4)	0.4 (4)
C5	0.4072 (6)	0.5135 (5)	0.1908 (3)	3.5 (5)	5.1 (6)	3.4 (4)	1.0 (5)	0.3 (4)	0.4 (4)
C6	0.3738 (6)	0.4452 (5)	0.2191 (3)	3.5 (5)	4.9 (6)	4.0 (5)	0.0 (4)	0.1 (4)	−0.3 (4)
C7	0.3004 (6)	0.3870 (5)	0.2947 (4)	3.5 (5)	5.1 (6)	5.9 (6)	−0.7 (5)	1.0 (5)	0.2 (5)
C8	0.2921 (7)	0.4022 (6)	0.3583 (4)	3.6 (6)	7.1 (7)	5.5 (6)	−0.8 (5)	2.4 (5)	1.2 (5)
C9	0.3922 (7)	0.3982 (5)	0.4021 (4)	6.3 (7)	4.2 (5)	5.7 (6)	−0.9 (5)	2.8 (6)	1.6 (4)
C10	0.5526 (6)	0.4623 (5)	0.4197 (3)	4.5 (5)	4.8 (5)	2.9 (4)	0.1 (5)	2.1 (4)	−0.0 (4)
C11	0.6124 (6)	0.5308 (5)	0.4191 (3)	3.9 (5)	4.4 (5)	2.8 (4)	−0.2 (5)	1.2 (4)	0.1 (4)
C12	0.5630 (6)	0.6045 (5)	0.4089 (3)	4.2 (5)	4.2 (5)	3.9 (5)	−0.6 (5)	2.0 (4)	−0.5 (4)
C13	0.3423 (8)	0.3723 (6)	0.1817 (4)	5.8 (7)	7.3 (7)	5.5 (6)	−1.5 (6)	1.0 (5)	−1.3 (5)
C14	0.5919 (7)	0.3970 (6)	0.4627 (4)	5.3 (6)	5.5 (6)	5.5 (6)	−0.5 (5)	1.6 (5)	1.3 (5)
C15	0.4312 (7)	0.5656 (6)	0.0919 (4)	5.7 (7)	6.6 (6)	4.5 (5)	0.7 (6)	1.1 (5)	0.7 (5)
C16	0.4524 (6)	0.5064 (5)	0.1409 (3)	3.6 (5)	5.4 (5)	2.9 (4)	0.2 (5)	0.3 (4)	0.2 (4)
C17	0.5571 (7)	0.4387 (6)	0.0837 (3)	5.8 (6)	8.5 (7)	2.1 (4)	0.9 (6)	1.0 (4)	0.0 (4)
C18	0.5875 (7)	0.3550 (6)	0.0770 (3)	6.5 (7)	8.6 (7)	2.2 (4)	0.4 (6)	1.7 (5)	−0.3 (4)
C19	0.6054 (6)	0.3283 (6)	0.1804 (3)	3.8 (5)	7.8 (7)	3.3 (5)	0.6 (5)	0.6 (4)	0.1 (5)
C20	0.5748 (7)	0.4094 (5)	0.1919 (3)	4.5 (6)	6.6 (7)	2.7 (4)	0.8 (5)	1.2 (4)	0.8 (4)
C21	0.7092 (7)	0.2549 (5)	0.1256 (4)	5.2 (6)	5.7 (6)	4.5 (5)	1.1 (5)	1.5 (5)	−1.1 (4)
C22	0.7882 (7)	0.2415 (5)	0.1836 (4)	4.1 (6)	5.3 (6)	4.4 (5)	2.2 (5)	1.3 (5)	−1.4 (4)
C23	0.7766 (7)	0.1834 (5)	0.2247 (4)	3.8 (6)	4.4 (5)	5.5 (6)	1.1 (5)	1.5 (5)	−0.2 (5)
C24	0.0788 (8)	0.1201 (6)	0.2087 (4)	6.2 (7)	6.0 (7)	5.7 (6)	0.9 (6)	2.0 (6)	−0.6 (5)
C25	0.6927 (8)	0.0650 (6)	0.2492 (5)	7.4 (8)	6.2 (7)	8.1 (8)	−0.2 (6)	3.1 (7)	−1.0 (6)
C26	0.7452 (10)	0.0724 (7)	0.3099 (5)	8.4 (9)	6.0 (7)	8.7 (8)	1.4 (7)	4.5 (7)	2.6 (6)
C27	0.8111 (9)	0.1303 (7)	0.3279 (4)	6.0 (7)	7.4 (8)	6.1 (7)	1.9 (7)	2.2 (6)	1.0 (6)
C28	0.8320 (7)	0.1877 (6)	0.2876 (4)	3.9 (5)	5.6 (6)	5.0 (5)	1.9 (5)	1.3 (5)	−0.1 (5)
C29	0.8961 (7)	0.2514 (5)	0.3053 (4)	3.8 (6)	5.7 (6)	4.1 (5)	2.3 (5)	0.8 (4)	−0.5 (4)
C30	0.9187 (7)	0.3043 (5)	0.2621 (4)	3.4 (5)	6.0 (6)	5.3 (6)	1.7 (5)	1.3 (5)	−1.7 (5)
C31	0.9901 (8)	0.3659 (7)	0.2766 (5)	4.3 (7)	7.4 (8)	6.2 (7)	−0.1 (6)	1.3 (5)	−2.3 (6)
C32	1.0086 (8)	0.4152 (6)	0.2352 (6)	4.6 (7)	5.2 (7)	10 (1)	−0.1 (6)	2.5 (7)	−1.3 (7)
C33	0.9537 (9)	0.4096 (6)	0.1744 (5)	6.8 (8)	5.9 (7)	7.6 (8)	1.2 (7)	3.6 (7)	1.1 (6)
C34	0.8834 (8)	0.3537 (6)	0.1580 (4)	4.3 (6)	6.8 (7)	6.1 (7)	0.2 (6)	1.8 (5)	−0.6 (6)
C35	0.8631 (7)	0.2994 (5)	0.2001 (4)	4.3 (6)	4.3 (5)	5.5 (6)	1.2 (5)	2.3 (5)	−0.8 (4)
C36	0.9317 (7)	0.2756 (6)	0.3715 (4)	4.2 (6)	6.9 (7)	5.3 (6)	1.5 (5)	0.3 (5)	−0.6 (5)
C37	0.9211 (7)	0.3879 (6)	0.4374 (4)	3.9 (6)	8.8 (8)	4.4 (5)	1.2 (5)	0.2 (5)	−1.0 (5)
C38	0.8813 (6)	0.4700 (6)	0.4360 (4)	2.6 (5)	8.2 (7)	4.2 (5)	0.6 (5)	−0.0 (4)	−0.9 (5)
C39	0.7302 (6)	0.4228 (5)	0.3651 (3)	3.9 (5)	5.8 (6)	2.9 (4)	−0.1 (5)	0.7 (4)	−0.8 (4)
C40	0.7750 (7)	0.3422 (6)	0.3700 (4)	4.2 (6)	8.8 (7)	4.5 (5)	0.4 (5)	1.5 (5)	−1.3 (5)
C41	0.7196 (6)	0.5308 (5)	0.4366 (3)	4.3 (5)	4.3 (5)	2.1 (4)	0.4 (4)	1.2 (4)	0.6 (4)
C42	0.7756 (7)	0.5939 (7)	0.4759 (4)	4.4 (6)	4.6 (5)	4.9 (5)	0.0 (5)	1.2 (5)	−0.0 (4)
CS1	0.4846 (12)	0.1379 (7)	0.3112 (6)	14.9 (14)	6.2 (8)	8.9 (9)	0.4 (9)	4.8 (9)	−0.5 (7)
CS2	0.5140 (10)	0.2198 (10)	0.3116 (5)	7.2 (9)	11.2 (1.2)	5.3 (7)	1.1 (9)	2.6 (6)	−0.6 (8)
NS1	0.5376 (9)	0.2850 (8)	0.3131 (5)	8.5 (8)	11.5 (9)	10.1 (8)	−0.1 (8)	2.9 (6)	−0.3 (8)
P1	0.3507 (2)	0.1685 (2)	0.4601 (1)	9.9 (2)	7.6 (2)	6.5 (2)	−2.5 (2)	3.8 (2)	−1.7 (1)
P2	0.3880 (2)	0.1127 (1)	0.1170 (1)	4.7 (1)	8.4 (2)	5.3 (1)	−1.1 (1)	1.6 (1)	−1.9 (1)
F1	0.3600 (7)	0.2442 (5)	0.4981 (4)	15.7 (8)	12.6 (7)	15.4 (8)	−1.0 (6)	4.6 (7)	−7.5 (6)
F2	0.2757 (7)	0.1334 (7)	0.4937 (4)	13.8 (8)	24.6 (12)	10.8 (6)	−8.7 (8)	5.5 (6)	−2.0 (7)
F3	0.4238 (8)	0.1311 (7)	0.5109 (6)	11.4 (8)	20.4 (12)	24.4 (14)	2.2 (8)	2.1 (8)	9.4 (10)
F4	0.4364 (9)	0.2005 (7)	0.4337 (5)	19.5 (11)	19.1 (10)	18.8 (10)	−6.7 (9)	12.8 (9)	−2.8 (8)
F5	0.3328 (12)	0.0955 (5)	0.4198 (5)	39.6 (20)	11.6 (7)	15.5 (9)	−6.8 (10)	14.8 (12)	−7.3 (7)
F6	0.2761 (13)	0.2071 (7)	0.4102 (6)	33.1 (19)	15.8 (10)	17.3 (10)	−2.0 (11)	−14.6 (12)	2.7 (8)
F7	0.4622 (10)	0.0698 (10)	0.1632 (5)	20.4 (12)	36.7 (20)	17.1 (10)	13.7 (1.3)	8.6 (9)	16.7 (13)
F8	0.4738 (5)	0.1379 (5)	0.0866 (3)	7.8 (5)	18.0 (8)	9.2 (5)	−2.5 (5)	3.7 (4)	1.1 (5)
F9	0.3750 (13)	0.0415 (9)	0.0775 (7)	29.1 (17)	24.5 (14)	25.6 (15)	−15.3 (13)	18.7 (14)	−19.2 (12)
F10	0.3161 (9)	0.1539 (15)	0.0663 (6)	13.1 (10)	56.9 (34)	18.6 (13)	15.8 (15)	1.7 (9)	9.0 (1.7)
F11	0.3055 (8)	0.0848 (5)	0.1490 (5)	18.6 (10)	14.0 (8)	28.9 (13)	−8.4 (7)	19.1 (10)	−8.3 (8)
F12	0.3938 (11)	0.1865 (5)	0.1528 (6)	35.5 (18)	10.0 (6)	25.3 (13)	−9.1 (9)	22.1 (1.4)	−8.3 (8)
CS3	0.157 (4)	0.389 (2)	0.006 (2)	37 (2)[d]					
CS4	0.258 (2)	0.385 (1)	0.006 (1)	20 (1)[d]					
NS2	0.328 (1)	0.399 (1)	0.0151 (8)	17.6 (7)[d]					

atom[c]	x	y	z	atom[c]	x	y	z
H1A	0.3542	0.6858	0.3941	H19A	0.6498	0.3071	0.2181
H1B	0.4740	0.7272	0.4063	H20A	0.5354	0.4071	0.2233
H2A	0.3691	0.7816	0.3212	H20B	0.6368	0.4412	0.2071

Table IV (*Continued*)

atom[c]	x	y	z	atom[c]	x	y	z
H2B	0.4609	0.7349	0.3025	H21A	0.6593	0.2105	0.1194
H3A	0.2626	0.6764	0.2853	H21B	0.7407	0.2574	0.0906
H3B	0.3113	0.7121	0.2321	H24	0.6713	0.1144	0.1661
H4	0.3689	0.6308	0.1778	H25	0.6466	0.0196	0.2364
H7A	0.2324	0.3837	0.2674	H26	0.7325	0.0329	0.3397
H7B	0.3356	0.3348	0.2930	H27	0.8465	0.1324	0.3717
H8A	0.2637	0.4557	0.3608	H31	1.0287	0.3729	0.3197
H8B	0.2477	0.3616	0.3704	H32	1.0620	0.4566	0.2463
H9A	0.3841	0.4049	0.4442	H33	0.9671	0.4483	0.1433
H9B	0.4233	0.3453	0.3983	H34	0.8466	0.3516	0.1151
H12	0.6018	0.6526	0.4266	H36A	0.9235	0.2285	0.3973
H13A	0.2858	0.3885	0.1470	H36B	1.0045	0.2885	0.3793
H13B	0.4002	0.3556	0.1653	H37A	0.9019	0.3579	0.4696
H13C	0.3189	0.3253	0.2005	H37B	0.9963	0.3906	0.4449
H14A	0.6560	0.3787	0.4533	H38A	0.9049	0.4942	0.4768
H14B	0.6066	0.4192	0.5044	H38B	0.9078	0.5022	0.4058
H14C	0.5504	0.3485	0.4631	H39A	0.6567	0.4186	0.3604
H15A	0.4961	0.5904	0.0884	H39B	0.7441	0.4505	0.3289
H15B	0.4023	0.5370	0.0526	H40A	0.7594	0.3136	0.4049
H15C	0.3843	0.6105	0.0935	H40B	0.7479	0.3123	0.3319
H17A	0.6165	0.4729	0.0876	H42A	0.8160	0.5674	0.5126
H17B	0.5054	0.4534	0.0464	H42B	0.8212	0.6187	0.4527
H18A	0.5271	0.3203	0.0698	H42C	0.7367	0.6368	0.4892
H18B	0.6190	0.3510	0.0418				

[a] Temperature factors have been multiplied by 10^2. [b] or *B*. [c] All hydrogens were generated by using X-RAY 72 hydrogen position generation program. The isotropic temperature factors for the generated hydrogen atoms were held constant at 4.0. [d] These atoms were refined by using isotropic temperature factors.

ervoir of 50 mL of boiling acetonitrile. The addition required 2 h, and the solution was stirred for an additional hour. The volume of the solution was reduced to 10 mL, and then 0.31 g (3.0 mmol) of triethylamine was added to the concentrated solution. The mixture was passed through an alumina column, using acetonitrile as an eluant, and the fastest moving band was recovered. The volume of the solution was reduced to 10 mL, and ethanol was added to induce crystallization; yield 0.34 g (30%). Anal. Calcd for $NiC_{34}H_{50}N_8P_2F_{12}$: C, 44.41; H, 5.48; N, 12.19. Found: C, 44.23; H, 5.69; N, 12.05.

(2,9,10,17,19,25,33,34-Octamethyl-3,6,13,16,20,24,27,31-octaazapentacyclo[16.7.7.2^{8,11}.2^{3,6}.2^{13,16}]hexatetraconta-1,8,10,17,19,24,26,31,33-nonaeneN$_4$)nickel(II) Hexafluorophosphate, [Ni{3,6-durene(CH$_2$piperazineEthi)$_2$Me$_2$[16]tetraeneN$_4$}](PF$_6$)$_2$. This reaction was performed as the preceding reaction, using 4.67 g (5.7 mmol) of [Ni{(piperazineEthi)$_2$Me$_2$[16]tetraeneN$_4$}](PF$_6$)$_2$ and 1.3 g (5.7 mmol) of bis(chloromethyl)durene; yield 1.98 g (35%). Anal. Calcd for $NiC_{38}H_{58}N_8P_2F_{12}$: C, 46.78; H, 5.99; N, 11.49; Ni, 6.02. Found: C, 46.67; H, 6.10; N, 11.37; Ni, 6.03.

(2,17,19,25-Tetramethyl-3,6,13,16,20,24,27,31-octaazaheptacyclo-[16.7.7.4^{9,10}.4^{33,34}.2^{3,6}.2^{8,11}.2^{13,16}]hexatetraconta-1,8,10,17,19,24,26,31,33,35,37,39,41-tridecaeneN$_4$)nickel(II) Hexafluorophosphate, [Ni{9,10-anthracene(CH$_2$piperazineEthi)$_2$[16]tetraeneN$_4$}](PF$_6$)$_2$. Two grams (2.4 mmol) of [Ni{(piperazinEthi)$_2$Me$_2$[16]tetraeneN$_4$}](PF$_6$)$_2$ and 0.62 (6.1 mmol) of triethylamine were added to 200 mL of acetonitrile. This solution was added slowly to a mixture of 0.68 g (2.6 mmol) of 9,10-bis(chloromethyl)anthracene in 100 mL of boiling acetonitrile. The addition required 2 h, and the mixture was stirred an additional 7 h. The mixture was filtered, and the volume was reduced to 10 mL. The filtrate was passed through an alumina column, using acetonitrile as an eluant, and the fastest moving band was recovered. The volume of the solution was reduced to 10 mL, the solution was filtered, and ethanol was added to induce crystallization. The crystals were ground to a powder and dried in vacuo at 80 °C; yield 1.18 g (47%). Anal. Calcd for $NiC_{42}H_{54}N_8P_2F_{12}$: C, 49.51; H, 5.53; N, 10.93. Found: C, 49.48; H, 5.34; N, 10.99.

(2,18,20,26-Tetramethyl-3,6,14,17,21,25,28,32-octaazapentacyclo-[17.7.7.2^{3,6}.2^{14,17}.1^{8,12}]hexatetraconta-1,8,10,12,18,20,25,27,32-nonaeneN$_4$)nickel(II) Hexafluorophosphate, [Ni{1,3-benzene(CH$_2$piperazineEthi)$_2$Me$_2$[16]tetraeneN$_4$}](PF$_6$)$_2$. Two grams (2.4 mmol) of [Ni{(piperazineEthi)$_2$Me$_2$[16]tetraeneN$_4$}](PF$_6$)$_2$ and 0.7 g (2.4 mmol) of 1,3-bis(bromomethyl)benzene were dissolved in 100 mL of boiling acetonitrile. The solution was stirred for 3 h and then reduced in volume in 10 mL. Seventy three hundredths gram (7.2 mmol) of triethylamine was added to the solution, which was filtered and passed through an alumina column, using acetonitrile as an eluant. The fastest moving band was recovered, and the volume of solution was reduced to dryness. The residue was dissolved in 350 mL of boiling methanol, and the methanol was slowly evaporated, inducing crystal formation; yield 0.39 g (17%). Anal. Calcd for $NiC_{34}H_{50}N_8P_2F_{12}\cdot 2CH_3OH$: C, 43.96; H, 5.94; N, 11.39. Found: C, 43.78; H, 5.85; N, 11.53.

2,6-Bis(chloromethyl)pyridine Hydrochloride. Five grams (36 mmol) of 2,6-bis(hydroxymethyl)pyridine was added to a 50-mL round-bottomed flask, and 10.7 g (85 mmol) of thionyl chloride was added slowly into the flask, resulting in vigorous gas evolution. Under a blanket of nitrogen, the slurry was heated, resulting in additional gas evolution and eventual solidification of the slurry. Fifteen milliliters of benzene was added, and the slurry was refluxed for 6 h. The slurry was filtered, and the gray precipitate was dissolved in 50 mL of hot ethanol. Upon cooling, precipitation occurred; yield 0.80 g (12%). No analytical data were acquired; compound identification was by loss of the OH stretch and appearance of a protonated pyridine in the infrared spectrum.

(2,18,20,26-Tetramethyl-3,6,14,17,21,25,28,32,34-nonaazapentacyclo[17.7.7.2^{3,6}.2^{14,17}.1^{8,12}]hexatetraconta-1,8,10,12,18,20,25,27,32-nonaeneN$_4$)nickel(II) Hexafluorophosphate, [Ni{(2,6-pyridine(CH$_2$piperazineEthi)$_2$Me$_2$[16]tetraeneN$_4$}](PF$_6$)$_2$. Two grams (2.4 mmol) of [Ni{(piperazineEthi)$_2$Me$_2$[16]tetraeneN$_4$}](PF$_6$)$_2$, 0.52 g (2.6 mmol) of bis(chloromethyl)pyridine hydrochloride, and 0.74 g (7.2 mmol) of triethylamine were dissolved in 100 mL of acetonitrile. The solution was heated to reflux and stirred for 4 h. The volume of the solution was reduced to 10 mL, and the solution was passed through an alumina column using acetonitrile as the eluant. The fastest moving band was recovered, the solution was reduced in volume to 10 mL, and methanol was added, inducing crystallization; yield 0.98 g (43%). Anal. Calcd for $NiC_{33}H_{52}N_9P_2F_{12}\cdot 1.5H_2O$: C, 41.83; H, 5.53; N, 13.31. Found: C, 41.92; H, 5.67; N, 13.16.

Synthesis of Carbon-13 Labeled Nickel(II) Compounds. (3,11-Diacetyl*-4,10-dimethyl-1,5,9,13-tetraazacyclohexadeca-1,3,9,11-tetraenatoN$_4$)nickel(II), [Ni(Ac*$_2$Me$_2$[16]tetraenatoN$_4$)]. To a solution of 1.94 g (6.37 mmol) of [Ni(Me$_2$[16]tetraenatoN$_4$)] and 1.61 g (16 mmol) of triethylamine dissolved in 200 mL of diethyl ether was added 1.0 g (1.27 mmol) of 90% carbon-13 enriched acetyl chloride. The solution immediately changed from clear purple to pale yellow with much voluminous orange precipitation. This precipitate was separated and washed with ether. The orange solid was dried and used without further purification. All manipulations were performed in an inert-atmosphere glovebox. No analyses were performed; yield: 2.45 g.

The labeled compounds described in the Results and Discussion were synthesized by techniques described earlier. No elemental analyses were performed.

Synthesis of the Chloride Salts of the Nickel(II) Complexes. (2,9,10,17,19,25,33,34-Octamethyl-3,6,13,16,20,24,27,31-octaazapentacyclo[16.7.7.2^{8,11}.2^{3,6}.2^{13,16}]hexatetraconta-1,8,10,17,19,24,26,31,33-nonaeneN$_4$)nickel(II) Chloride, [Ni{3,6-durene(CH$_2$piperazineEthl)$_2$Me$_2$-[16]tetraeneN$_4$}](Cl)$_2$. One gram (1.0 mmol) of [Ni{3,6-durene(CH$_2$piperazineEthi)$_2$Me$_2$[16]tetraeneN$_4$}](PF$_6$)$_2$ was dissolved in 20 mL of acetone and 1.5 g (5.3 mmol) of tetrabutylammonium chloride, dissolved

in 10 mL of acetone, was dripped slowly into the nickel(II) solution. A voluminous yellow precipitate formed immediately and was recovered and dried in vacuo. The dried precipitate was dissolved in a minimum amount of acetonitrile, and acetone was added to induce crystallization. The crystalline product was dried in vacuo at room temperature; yield 0.34 g (44%). Anal. Calcd for $NiC_{38}H_{58}N_8Cl_2 \cdot 5.5H_2O$: C, 53.34; H, 8.13; N, 13.10; Cl, 8.29. Found: C, 53.03; H, 8.01; N, 12.84; Cl, 8.69.

(2,17,19,25-Tetramethyl-3,6,13,16,20,24,27,31-octaazapentacyclo-[16.7.7.2^{8,11}.2^{3,6}.2^{13,16}]hexatetraconta-1,8,10,17,19,24,26,31,33-nonaeneN$_4$)nickel(II) Chloride, [Ni{1,4-benzene(CH$_2$piperazineEthi)$_2$Me$_2$-[16]tetraeneN$_4$}](Cl)$_2$. This reaction was performed as the preceding reaction, using 0.3 g (0.32 mmol) of [Ni{1,4-benzene(CH$_2$piperazine-Ethi)$_2$Me$_2$[16]tetraeneN$_4$}](PF$_6$)$_2$ dissolved in 10 mL of acetone and 0.3 g (1.1 mmol) of tetrabutylammonium chloride dissolved in 5 mL of acetone; yield 0.16 g (70%). Anal. Calcd for $NiC_{34}H_{50}N_8Cl_2 \cdot CH_3COCH_3 \cdot 3H_2O$: C, 55.79; H, 7.85; N, 14.07; Cl, 8.90. Found: C, 55.46; H, 8.08; N, 14.68; Cl, 8.10.

(2,18,20,26-Tetramethyl-3,6,14,17,21,25,28,32-octaazapentacyclo-[17.7.7.2^{3,6}.2^{14,17}.1^{8,12}]hexatetraconta-1,8,10,12,18,20,25,27,32-nonaeneN$_4$)nickel(II) Chloride, [Ni{1,3-benzene(CH$_2$piperazineEthi)$_2$Me$_2$-[16]tetraeneN$_4$}](Cl)$_2$. This reaction was performed as the preceding reaction, using 0.25 g (0.26 mmol) of [Ni{1,3-benzene(CH$_2$piperazine-Ethi)$_2$Me$_2$[16]tetraeneN$_4$}](PF$_6$)$_2$ dissolved in 10 mL of acetone and 0.25 g (0.9 mmol) of tetrabutylammonium chloride dissolved in 5 mL of acetone; yield 0.095 g (50%). Anal. Calcd for $NiC_{34}H_{50}N_8Cl_2 \cdot H_2O$: C, 56.84; H, 7.30; N, 15.60; Cl, 9.87. Found: C, 56.74; H, 7.30; N, 15.57; Cl, 10.91.

(2,17,19,25-Tetramethyl-3,6,13,16,20,24,27,31-octaazaheptacyclo-[16.7.7.4^{9,10}.4^{33,34}.2^{3,6}.2^{8,11}.2^{13,16}]hexatetraconta-1,8,10,17,19,24,26,31,33,35,37,39,41-tridecaeneN$_4$)nickel(II) Chloride, [Ni{9,10-anthracene (CH$_2$piperazineEthi)$_2$ Me$_2$[16]tetraeneN$_4$}](Cl)$_2$. Two-tenths of a gram (0.2 mmol) of [Ni{9,10-anthracene(CH$_2$piperazineEthi)$_2$Me$_2$[16]tetrae-neN$_4$}](PF$_6$)$_2$ was dissolved in 20 mL of acetone and 0.25 g (0.5 mmol) of tetrabutylammonium chloride, dissolved in 20 mL of acetone, was slowly added to the nickel(II) solution. The resulting voluminous precipitate was recovered and dried in vacuo. The preceding steps were performed in an inert-atmosphere glovebox. The precipitate was removed from the glovebox and dissolved in a small amount of acetonitrile. Sufficient acetone was added to induce crystallization, and the recovered crystalline product was dried in vacuo at room temperature; yield 0.044 g (25%). Anal. Calcd for $NiC_{42}H_{54}N_8Cl_2 \cdot 5H_2O$: C, 56.64; H, 7.24; N, 12.58; Cl, 7.96. Found: C, 56.85; H, 7.16; N, 12.17; Cl, 7.88.

Physical Measurements. Elemental analyses were performed by Galbraith Laboratories, Inc., Knoxville, TN. Infrared spectra were obtained from 4000 to 200 cm^{-1} with use of a Perkin-Elmer Model 283B infrared spectrophotometer. Samples were ground and then mulled with Nujol. Proton NMR spectra were acquired by using several instruments: two continuous-wave spectrometers, a Varian EM360L (60 MHz) and a Varian EM390 (90 MHz); two Fourier transform spectrometers, a Bruker WH90 (90 mHz) and a Bruker WM300 (300 MHz). Carbon-13 NMR spectra were acquired by using two Fourier transform spectrometers: a Bruker WP80 (30 MHz) and a Bruker WM300 (75 MHz). All NMR spectra were obtained on samples dissolved in deuterated solvents.

Crystal Measurements. A suitable crystal of [Ni{9,10-anthracene-(CH$_2$piperazineEthi)$_2$Me$_2$[16]tetraene$_4$}](PF$_6$)$_2$·2CH$_3$CN, of dimensions 0.2 × 0.5 × 0.2 mm, was selected and mounted on a thin quartz fiber by using "Araldite" epoxy resin. The crystal and fiber were mounted on a Syntex $P2_1$ four-circle automated diffractometer. Twelve high-angle reflections yielded the cell parameters: a = 13.798 (3) Å, b = 16.976 (3) Å, c = 22.769 (6) Å, V = 5185.1 (2.1) Å^3, β = 103.55 (2)°. The calculated density, ρ_{calcd} = 1.40 g cm^{-3}, for N = 4 agrees well with the observed density, ρ_{obsd} = 1.42 g cm^{-3}, from crystal flotation in a cyclohexane/bromoform mixture.

With use of x-radiation of wavelength $\lambda_{MoK\alpha}$ = 0.7107 Å, intensity data were collected using the ω–2θ scan technique, ±0.85° from the $K\alpha_1$–$K\alpha_2$ position, for all data between 2θ = 0° and 50°. A variable scan rate was used, 2–29° min^{-1}, depending on the intensity of a 2-s prescan. Backgrounds were measured at each end of the scan for 0.25 of the scan time. The crystal was held at 16 (0.5) °C with the Syntex LT-1 attachment.

To monitor crystal decay, three standard reflections were examined every 100 reflections. Some irregularity was detected, but no secular trend, so no corrections were effected. No absorption corrections were performed, for the crystal was small and the measured absorption coefficient, μ, was 5.14 cm^{-1}.

A total of 6459 reflections were examined, where 3697 were independent and possessed $I/\sigma(I) \geq 3.0$ values. These $3\sigma(I)$ data were used in refinement and corrected for Lorenz and Polarization factors. From the systematic absences, $0k0$ for k = odd and $h0l$ for $h + l$ = odd, the space group was uniquely determined as the centrosymmetric space group $P2_1/n$, a nonstandard setting of the conventional space group $P2_1/c$.

Solution and Refinement of the Structure. The structure was solved by the heavy-atom method. The locations of the nickel atoms and the two phosphorus atoms were deduced from a three-dimensional Patterson map. The locations of the remaining non-hydrogen atoms were determined from subsequent difference Fourier maps and were refined by least-squares methods. The crystal structure was initially solved by using the CRYM system and then refined by using the X-RAY 72 system of X-ray structure computing programs.

With use of the X-RAY 72 system, all non-hydrogen atoms, with the exception of the nonassociated acetonitrile molecule, were given anisotropic temperature factors, and their positions were refined by full-matrix least-squares calculations. During the final cycles of least-squares calculations, all hydrogen atom positions were included as fixed calculated contributions. Minimizing the function $R(F) = \sum w(|F_o| - |F_c|)^2$ and utilizing the weighting function $w = 1.0/(1 - [(F_o - B)/A]^2)$, the refinement converged, yielding the final disagreement indices: R = 7.4%, R^1 = 9.9%, and GOF = 1.97.

A weighing analysis showed no significant correlation between F_o, (sin θ)/λ, and the average $w(|F_o| - |F_c|)^2$ values, justifying the weighting function listed above. A final difference Fourier map showed that all electron density was considered in the refinement. Finally, the maximum shift/σ value for all atomic parameters was 0.23, suggesting that the refinement was complete.

Table IV presents the coordinates for the atoms and the temperature factors.

Acknowledgment. The support of the National Science Foundation and the National Institutes of Health is gratefully acknowledged. KJT is appreciative of fellowships from the Sohio Corporation and from The Ohio State University. Contributions to the preparation of this manuscript by the staff of the Cooperative Institute for Research in the Environmental Sciences, University of Colorado, Boulder is also appreciated very much.

Registry No. V (R = 1,4-benzene)(PF$_6$)$_2$, 85630-87-1; V (R = 3,6-durene)(PF$_6$)$_2$, 85630-88-2; V (R = 9,10-anthracene)(PF$_6$)$_2$, 77424-23-8; V (R = 1,3-benzene)(PF$_6$)$_2$, 85630-90-6; V (R = 2,6-pyridine)(PF$_6$)$_2$, 85630-92-8; V (R = 3,6-durene)(Cl)$_2$, 85630-93-9; V (R = 1,4-benzene)(Cl)$_2$, 85630-94-0; V (R = 1,3-benzene)(Cl)$_2$, 85630-95-1; V (R = 9,10-anthracene)(Cl)$_2$, 85630-96-2; V (R = 9,10-anthracene)-(PF$_6$)$_2$·2CH$_3$CN, 85630-97-3; VI, 70021-28-2; VII, 77424-20-5; piperazine, 110-85-0; *p,p*-bis(chloromethyl)benzene, 623-25-6; bis(chloromethyl)durene, 3022-16-0; 9,10-bis(chloromethyl)anthracene, 10387-13-0; 1,3-bis(bromomethyl)benzene, 626-15-3; bis(chloromethyl)pyridine hydrochloride, 55422-79-2.

Supplementary Material Available: A listing of structure factors for [Ni{9,10-anthracene(CH$_2$piperazineEthi)$_2$Me$_2$[16]tetra-eneN$_4$}](PF$_6$)$_2$·2CH$_3$CN (15 pages). Ordering information is given on any current masthead page.